Level spectrum of ^{219}Ra and weak coupling in the light actinide region

P. D. Cottle,* M. Gai, J. F. Ennis,† J. F. Shriner, Jr.,‡ and D. A. Bromley
A.W. Wright Nuclear Structure Laboratory, Yale University, New Haven, Connecticut 06511

C. W. Beausang, L. Hildingsson,§ W. F. Piel, Jr., and D. B. Fossan
Department of Physics, State University of New York, Stony Brook, New York 11794

J. W. Olness and E. K. Warburton
Department of Physics, Brookhaven National Laboratory, Upton, New York 11973
(Received 14 August 1987)

We present a level spectrum for ^{219}Ra derived from data on the reaction ^{208}Pb(^{14}C,3n) studied at beam energies near the Coulomb barrier. Measurements of γ-ray excitation functions, γ-γ coincidences, γ-ray angular distributions, and electron conversion coefficients were made. The ground state band shows an alternating parity structure and is consistent with an interpretation in terms of a $g_{9/2}$ neutron weakly coupled to an even-even core. A nonyrast side band is observed and may arise from the anomalous coupling of a $j_{15/2}$ neutron to the core. The dependence of particle-core coupling behavior on the quadrupole deformation of the core and on the orbital in which the odd nucleon is located is discussed.

I. INTRODUCTION

Nuclear structure studies have provided a well developed understanding of the coupling mechanism between an unpaired valence nucleon and an even-even core nucleus when the core is either spherical or has a well-deformed prolate shape. For nuclei that lie in regions of transition between these two limits, however, the particle-core coupling behavior is not as well understood. In particular, the range of deformations in which a weak coupling-like description[1] can be applied is not clear, nor is the role played by the characteristics of the single valence particle orbital.

A number of experimental studies[2–15] have mapped the transition from spherical to quadrupole deformed nuclear shapes in even mass isotopes of radium and thorium. Results of these studies reveal that this shape transition is of a gradual nature,[8,16] in contrast to the more abrupt changes observed in a number of other nuclear transition regions.[17] The gradual character of the transition in the $Z=88-90$ region offers an excellent opportunity for study of the weak-to-strong particle-core coupling transition in odd-mass nuclei.

In this article, we present the results of an experimental study of ^{219}Ra in which bands of states built on two different single neutron orbitals are observed. The excitation spectrum of this nucleus is discussed in terms of a weak coupling description, and the applicability of such a model to other odd-A nuclei in this region is considered. Finally, we are able to observe, using data from this study and from studies of odd-A neighbors, the evolution of particle-core coupling behavior as a function both of the core deformation and of the single particle orbital occupied by the unpaired nucleon. One other study of high spin states of ^{219}Ra has been reported;[18] its results are completely consistent with ours but more limited in scope. A preliminary version of the present work was published earlier.[19]

II. EXPERIMENTAL PROCEDURE

The nucleus ^{219}Ra was studied via the ^{208}Pb(^{14}C,3n)^{219}Ra reaction, using the ^{14}C beam from the Brookhaven National Laboratory MP-7 tandem Van de Graaff accelerator. Experimental measurements included γ-ray excitation functions, γ-γ coincidences, γ-ray angular distributions, and conversion electrons.

Both thick (50 mg/cm^2) and thin (300 μg/cm^2 on 225 μg/cm^2 Au) targets of enriched ^{208}Pb were employed for the excitation function measurements. Gamma radiation was detected at 90° to the beam in a Ge(Li) detector. Beam energies ranged from 60 to 78 MeV; over this energy range the primary evaporation residues are ^{220}Ra, ^{219}Ra, and ^{218}Ra, corresponding to the 2n, 3n, and 4n channels, respectively. The thin target excitation curve measurement showed quite clearly the characteristic Ghoshal pattern of (HI,xn) cross sections for the strong 3n and 4n channels (see Fig. 1). Detailed information on ^{218}Ra and alpha particle decay data for ^{220}Ra were available, so that the combination of excitation curve measurements and x-ray coincidence data was sufficient to identify the strongest gamma-rays deexciting states of ^{219}Ra. Furthermore, the beam energies at which these gamma rays were most intense matched quite well those calculated using the computer code PACE.[20]

Gamma-gamma coincidence data were taken with the thick (50 mg/cm^2) ^{208}Pb target at a beam energy of 68 MeV using one n-type Ge detector of 20% efficiency and two Ge(Li) detectors of 22% and 19% efficiency; their resolutions were 2.0–2.1 keV full width at half maximum (FWHM) at 1.33 MeV. The use of a thick target allowed the observation of reactions occurring at energies from the beam energy down to the Coulomb barrier.

This enhanced the population of lower spin states and allowed the identification of a non-yrast side band weakly populated in this reaction. A total of 2.5×10^8 coincidence events was collected and recorded on event tapes for off-line analyses.

The gamma-ray angular distribution measurements were performed using the thick target at a beam energy of 67 MeV. Two detectors were used—the first a Compton-suppression spectrometer (CSS) consisting of an n-type Ge detector inside a 25.4×20.3-cm NaI(Tl) crystal and the second a low energy photon spectrometer (LEPS). Data were taken at six angles between 0° and 90° with each detector. Typical beam currents were 4 particle nA, and data were acquired for approximately 8 h at each angle. Spectra from both the LEPS and CSS are shown in Fig. 2. The LEPS was used for measurements of gamma rays below 400 keV because of its superior resolution (0.7 keV FWHM at 122 keV). For gamma rays above 400 keV, however, the CSS was used because of its higher efficiency in this energy range.

To establish the magnetic or electric nature of transitions, conversion electrons were studied using a mini-orange electron spectrometer.[21] The large difference in conversion coefficients characteristic of electric and magnetic dipole transitions in this region[22] makes this measurement particularly sensitive to the nature of these transitions; at 250 keV the K conversion coefficient for an $M1$ transition is 23 times larger than that for an $E1$ transition. The magnetic filter in the mini-orange spectrometer consisted of five permanent samarium cobalt magnets arranged symmetrically around a central lead plug. The electron energies were measured using a Si(Li) detector at 125° to the beam direction. A portion of the resulting electron spectrum is shown in Fig. 3.

III. EXPERIMENTAL RESULTS

Coincidence spectra were generated using all detected gamma rays; several spectra gated on gamma rays in ^{219}Ra are shown in Fig. 4. The angular distribution of each gamma ray was fitted to

$$W(\theta)=A_0[1+A_2P_2(\theta)+A_4P_4(\theta)] .$$

The experimental values of A_2 and A_4 are listed in Table I for each gamma ray in ^{219}Ra together with its relative intensity and assigned location in the level spectrum.

We have assumed a tentative ground state spin assignment based on an examination of the systematic behavior of ground state spins in neighboring odd-N, even-Z nuclei[15,23–28] (see Fig. 5). For $N<134$, the ground state spins appear to be the same within each set of isotones.[15] Based on the $\frac{9}{2}^+$ ground state spin assignment for ^{217}Rn, we suggest the same spin and parity for the ground state of ^{219}Ra. In the report of their study of ^{219}Ra by the alpha particle decay of ^{223}Th, El-Lawindy *et al.*[29] suggest that the ground state spin of ^{219}Ra is $\frac{7}{2}^+$; however, their data do not allow them to rule out the assignments of $\frac{9}{2}^+$ or $\frac{11}{2}^+$ for this state.

To make spin assignments for states in the ground state rotational band, the usual assumption for (HI,xn) reactions in heavy nuclei[30]—that intraband transitions are stretched—was adopted. In such cases, dipole transitions have negative A_2 values and quadrupole transitions positive A_2 values; with such an assumption, the measured angular distributions permit straightforward spin assignments for the band members.

To extract values for the conversion coefficients for the ground state band, the electron peaks were fitted using a modified Gaussian function. The peak areas were corrected for the relative efficiency of the mini-orange spectrometer, which was measured out of beam using a thin ^{152}Eu source. Absolute values for the conversion coefficients were then obtained by dividing by the known gamma-ray intensities and using one of the strong yrast band $E2$ transitions (the 295-keV $\frac{17}{2}^+\rightarrow\frac{13}{2}^+$ transition) to normalize the data.

The fit to the region around the $K295$ peak is shown in Fig. 6. This broad peak actually contains several conversion lines, the strongest being $K295$. From this group of peaks, we obtain an upper limit $\alpha_L(205)/\alpha_K(295)\leq0.27$. This result can be compared with calculated conversion coefficients of 0.20 if the 205 keV transition

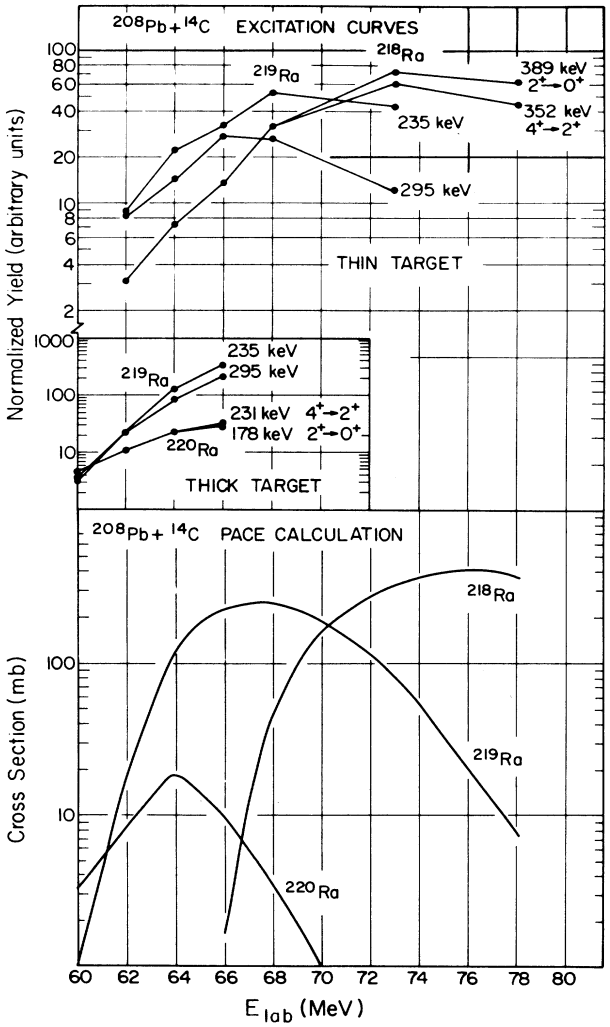

FIG. 1. Excitation function measurement results for thin and thick targets (top) and a calculation using the PACE code (bottom).

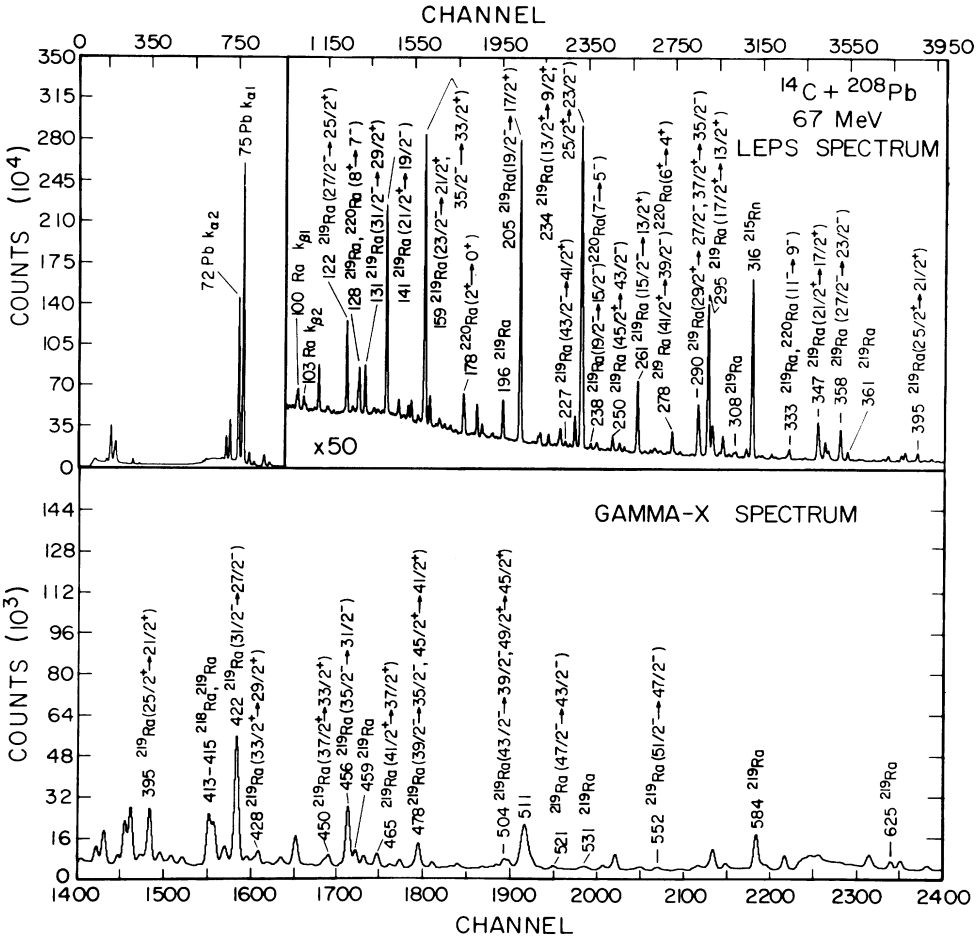

FIG. 2. Spectra from the two detectors used in the angular distribution experiment: top—LEPS spectrum; bottom—n-type Ge (gamma-x) Compton-suppressed spectrum.

was $E1$ and 4.47 if it was $M1$ in nature;[22] therefore, it was concluded that the 205-keV transition is $E1$. In all, conversion coefficients were extracted for ten transitions in ^{219}Ra, including six interband dipole transitions. These results are summarized in Table II and are presented in graphical form in Fig. 7. Each conversion coefficient measured for a dipole transition is consistent with the value expected for an $E1$ transition and definitely rules out an $M1$ character, thus establishing the alternating parities shown in our final proposed level spectrum (Fig. 8).

Only tentative spin and parity information could be extracted for the weakly populated side-band members; the results obtained are, however, supported by intensity arguments. Such arguments allow us to deduce that the 128.7 keV transition must have an $E1$ multipolarity. We conclude that the 414 keV gamma ray, under the assumption of stretched intraband transitions and the long mean life expected for an $M2$ transition of this energy, must be of $E2$ character. Further, we expect from the behavior of other states in our study that the feeding of the 128.7 keV level by the 414.0 keV transition accounts for most of the population of this state. The conversion coefficients for 128.7 keV gamma rays of $E1$, $E2$, $M1$, and $M2$ multipolarities are 0.24, 3.24, 7.93, and 47.8, respectively.[22] Since the 128.7 keV gamma ray has $I_\gamma = 67$ (see Table I), these multipolarities would yield, respectively, $I_{tr} = 69$, 235, 494, and 2702 (compared to a value of $I_{tr} = 52$ for the 414 keV transition). Clearly, only an $E1$ multipolarity is consistent with our expectation concerning the feeding of the 128.7 keV state.

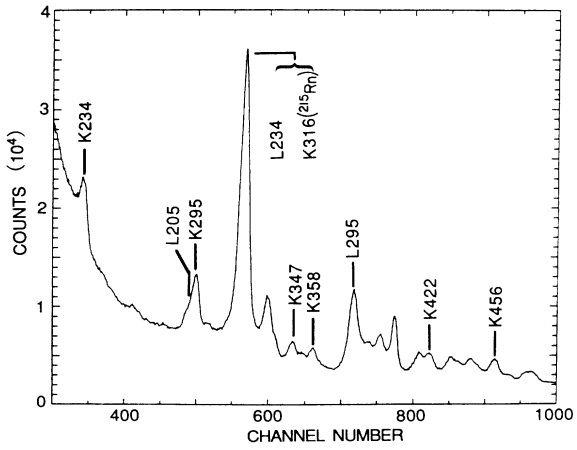

FIG. 3. Conversion electron spectrum from the mini-orange spectrometer. A number of lines from ^{219}Ra are labeled.

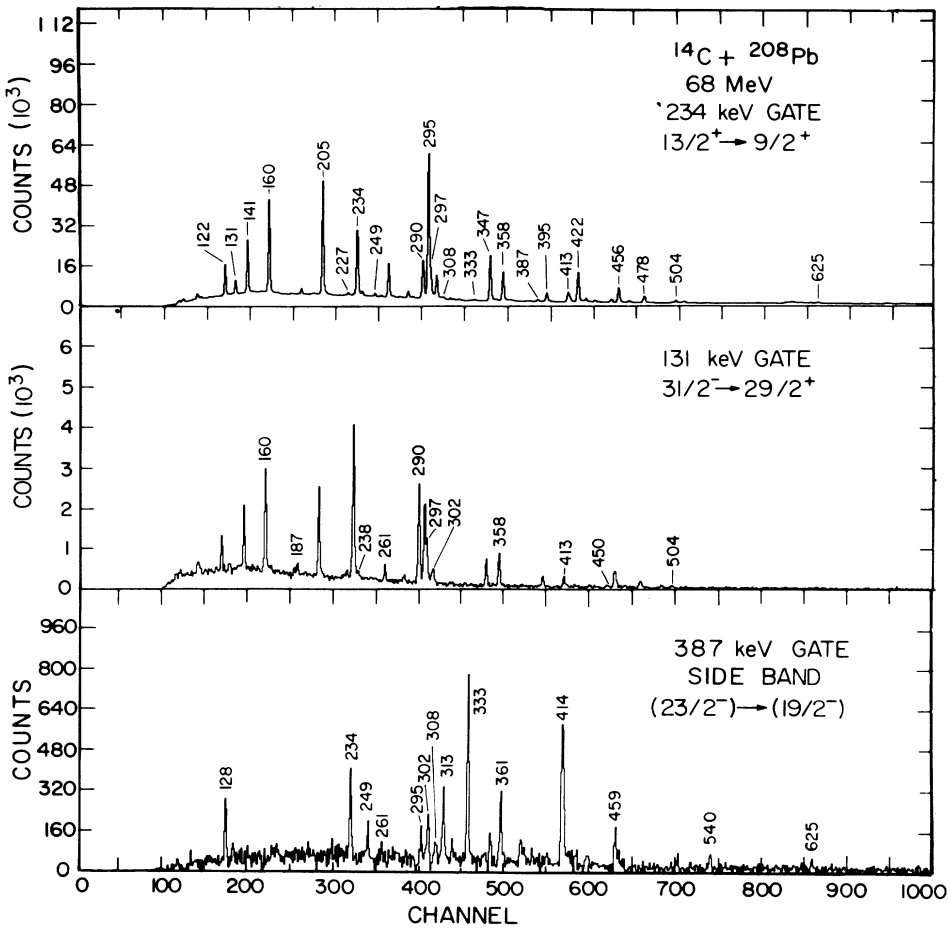

FIG. 4. Gamma-ray spectra gated on several transitions from ^{219}Ra. Both the 234 and 131 keV deexcitations are located in the alternating parity band based on the ground state. The 387 keV deexcitation is found in the side band.

The existence of the transition from the 1263.7 keV level to the 1035.6 keV level was deduced from the observation of transitions in the ground state band above the 495.4 keV level in spectra gated on gamma rays in the side band above the 1263.7 keV level. We did not observe a 227 keV gamma ray in spectra gated on the appropriate side band transitions; therefore, we conclude that this transition has a large electron conversion coefficient. For a 227 keV gamma ray, conversion coefficients are 0.054 for $E1$, 0.397 for $E2$, 1.72 for $M1$, and 7.04 for $M2$.[22] Since a 227 keV $M2$ transition would be very slow, the 227 keV transition is probably $M1$. The determination of this multipolarity places a constraint on the possible spins of the 1263.7 keV level.

Finally, since the 414.0 keV, 333.6 keV, and 387.4 keV gamma rays appear—from angular distribution data—to be stretched $E2$ transitions, the constraints that we have already mentioned require that the 128.7 keV level have $J^\pi = \frac{11}{2}^-$. This conclusion is consistent with the observed angular distribution of the 128.7 keV gamma ray. Each of these spin assignments is listed as tentative, however, because of their dependence on intensity arguments.

Where the presence of gamma-ray doublets make the determination of intensities from angular distribution data impossible, they were deduced from coincidence information.

Recently, much attention has been focused on the importance of electric dipole transition matrix elements in making inferences concerning the structure of nuclei in

Z \ N	127	129	131	133	135	137	139	141
^{82}Pb	9/2$^+$	(9/2$^+$)						
^{84}Po	9/2$^+$	9/2$^+$	(9/2$^+$)					
^{86}Rn	(9/2$^+$)	(9/2$^+$)	9/2$^+$	(5/2$^+$)	(7/2$^+$,9/2$^+$)			
^{88}Ra	(9/2$^+$)	(9/2$^+$)	(9/2$^+$)	5/2$^+$	3/2$^+$	1/2$^+$	3/2$^+$	5/2$^+$
^{90}Th					(3/2$^+$)	(3/2$^+$)	5/2$^+$	5/2$^{(+)}$
^{92}U						(3/2$^+$)	(5/2$^-$)	5/2$^+$

GROUND STATE SPINS $Z \geq 82$

FIG. 5. Ground state spins of even-Z, odd-N nuclei in the $Z = 82$–92 region (Refs. 15 and 23–28). Assignments shown in parentheses are tentative.

TABLE I. Characteristics of ^{219}Ra gamma radiation.

E_γ(keV)[a]	$A2$	$A4$	I_γ [b]	I_{tr} [c]	$2x\,(J_i^\pi \rightarrow J_f^\pi)$
122.5	−0.27(1)		145(7)	155(8)	$27^- - 25^+$
128.7	−0.24(1)		67(3)	69(3)	$(11^-) - 9^+$
131.4	−0.27(1)		77(4)	79(4)	$(31^-) - 29^+$
141.5	−0.27(1)		327(16)	324(16)	$21^+ - 19^-$
159.6[d]			433(22)	408(20)	$23^- - 21^+$
159.6[d]			72(10)	68(9)	$35^- - 33^+$
187.7	−0.25(2)		22(1)	20(1)	$39^- - 37^+$
196.3	0.23(1)	0.11(1)	101(5)	90(5)	
205.1	−0.22(1)		679(34)	600(30)	$19^- - 17^+$
226.8	−0.23(7)		16(2)	14(2)	$43^- - 41^+$
231.9[e]			14(3)	12(2)	$49^+ - 47^-$
234.3[d]			1206(60)	1336(67)	$13^+ - 9^+$
234.5[d]			196(23)	170(20)	$25^+ - 23^-$
238.3	0.47(4)	−0.17(6)	19(1)	20(1)	$19^- - 15^-$
249[d,g]			19(2)		
249.5[d]			33(4)	29(4)	$45^+ - 43^-$
261.1	−0.23(1)		263(13)	226(11)	$15^- - 13^+$
270.7[e]			6(2)	5(1)	$47^- - 45^+$
277.7[e]			45(7)	38(6)	$41^+ - 39^-$
290.4[d]			196(10)	167(8)	$29^+ - 27^-$
290.7[d]			102(5)	87(4)	$37^+ - 35^-$
294.8[d]			1000(50)	1000(50)	$17^+ - 13^+$
295[d,g]			37(3)		
297.3	−0.12(1)		188(9)	160(80)	$33^+ - 31^-$
301.9[d]			138(7)	129(6)	$23^- - 19^-$
302[d,g]			8(1)		
307.7[g]			24(1)		
308.6	−0.21(6)		24(1)	20(1)	$(15^-) - 13^+$
313[e,g]			28(2)		
320.7	−0.18(8)		16(1)	13(1)	$51^- - 49^+$
333.6	0.28(7)	0.01(10)	69(4)	66(3)	$19^- - 15^-$
347.5	0.20(1)	−0.08(1)	404(20)	364(18)	$21^+ - 17^+$

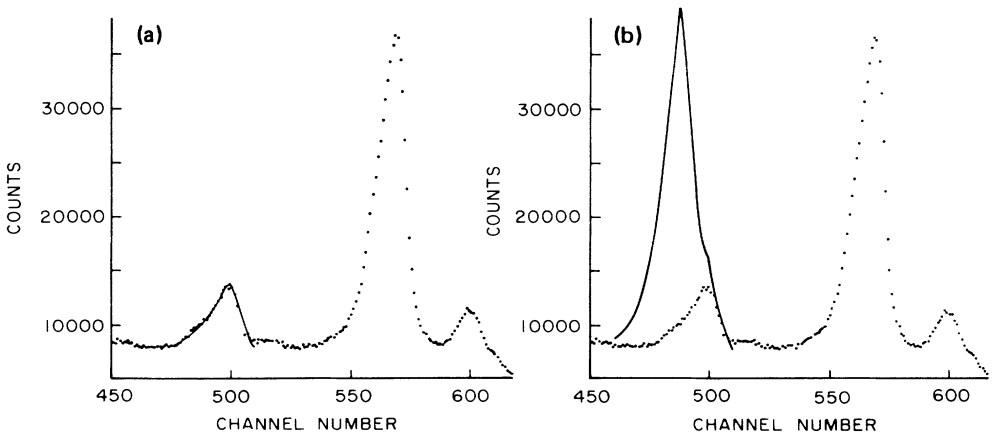

FIG. 6. Two fits to the conversion electron spectrum near the $K295$ peak. The broad structure on the left side of the spectrum contains not only the $K295$ peak, but also the $K290$, $L205$, and $K297$ ones; the $K290$ and $L205$ peaks form an exact doublet. Panel (a) shows the best fit. The ratio of the area of the sum peak ($L205+K290$) to the $K295$ peak gives an upper limit for the ratio of the conversion coefficients $\alpha_L(205)/\alpha_K(295) \leq 0.27$. If the 205 keV gamma ray is $E1$, then this ratio (Ref. 22) would have the value 0.20; if it were $M1$, the ratio would be 4.47. Panel (b) shows the fit that would be expected if this line were $M1$, emphasizing the large difference in $E1$ and $M1$ conversion coefficients in this region.

TABLE I. (*Continued*).

E_γ(keV)[a]	$A2$	$A4$	I_γ[b]	I_{tr}[c]	$2x(J_i^\pi \rightarrow J_f^\pi)$
358.0	0.30(1)	−0.11(1)	309(15)	276(14)	$27^- - 23^-$
361.4	0.36(2)	−0.09(3)	77(4)	69(3)	$(27^-) - (23^-)$
387.4	0.30(2)	−0.18(3)	74(4)	66(3)	$(23^-) - (19^-)$
395.0	0.40(2)	−0.22(3)	92(5)	81(4)	$25^+ - 21^+$
413.1[d,f]			27(6)	24(5)	$29^+ - 25^+$
414.0[d,f]			60(15)	52(13)	$(15^-) - (11^-)$
415.1[d,f]			15(8)	13(7)	$(31^-) - (27^-)$
422.0	0.31(1)	−0.13(1)	251(13)	215(11)	$31^- - 27^-$
428.7	0.73(4)	−0.45(10)	22(1)	19(1)	$33^+ - 29^+$
450.2[i]	0.24(2)		30(2)	26(1)	$37^+ - 33^+$
456.5	0.34(1)	−0.19(2)	126(6)	107(5)	$35^- - 31^-$
458.6[g]	−0.25(3)	−0.01(5)	55(3)		
465.4	0.23(2)	−0.16(6)	33(2)	28(1)	$41^+ - 37^+$
476.9[d]			12(3)	10(3)	$45^+ - 41^+$
478.7[d]			37(3)	31(3)	$39^- - 35^-$
503.7[i]	0.41(8)		12(1)	10(1)	$49^+ - 45^+$
505.0[i]	−0.01(6)		16(1)	14(1)	$43^- - 39^-$
520.7	0.02(10)	−0.11(19)	6(1)	5(1)	$47^- - 43^-$
530.8[g,h]			<3		$(53^+) - 49^+$
552.4	−0.02(12)	0.44(32)	5(2)	4(1)	$51^- - 47^-$
584.7[g,h]			<3		
625.9[g]	−0.27(4)	−0.03(7)	37(2)		

[a]Energies are accurate to 0.2 keV.
[b]Bare gamma ray intensity relative to 294.8 keV gamma ray.
[c]Intensity (including internal conversion) relative to 294.8 keV transition.
[d]Doublet in ^{219}Ra.
[e]Doublet in ^{220}Ra.
[f]Doublet in ^{218}Ra.
[g]Multipolarity unknown.
[h]Doublet with unassigned gamma ray.
[i]Only three angles available because of problems fitting this peak; therefore, only second order Legendre polynomial used.

this region.[31,32] Our measurements yield values of $B(E1{:}J \rightarrow J-1)/B(E2{:}J \rightarrow J-2)$ for the ground state band as listed in Table III.

IV. DISCUSSION

All three of the low-lying single neutron states observed[15] in ^{209}Pb are also seen[33] in ^{217}Ra; therefore, one might expect to observe these relatively pure configurations in ^{219}Ra as well. The assumed $\frac{9}{2}^+$ ground state spin and parity of ^{219}Ra is consistent with a $\nu g_{9/2}$ configuration. We conclude that we have not observed the $\nu i_{11/2}$ configuration because of the absence of $J^\pi = \frac{11}{2}^+$ states from the spectrum. Two $J^\pi = \frac{15}{2}^-$ states are, however, available as candidates for the assignment of the $\nu j_{15/2}$ configuration. The lower of these appears to belong to a negative parity band which shows enhanced $E1$ deexcitations (see Table III) and probably results from the weak coupling of a $g_{9/2}$ neutron to the 3^- state of the ^{218}Ra core nucleus.[5] Branching ratios of gamma-ray deexcitations from members of this band yield an average value of $B(E1;J \rightarrow J-1)/B(E2;J \rightarrow J-2)$ of 2.1×10^{-6} fm^{-2}. If we estimate that the $E2$ deexcitations connecting members of this band have[10]

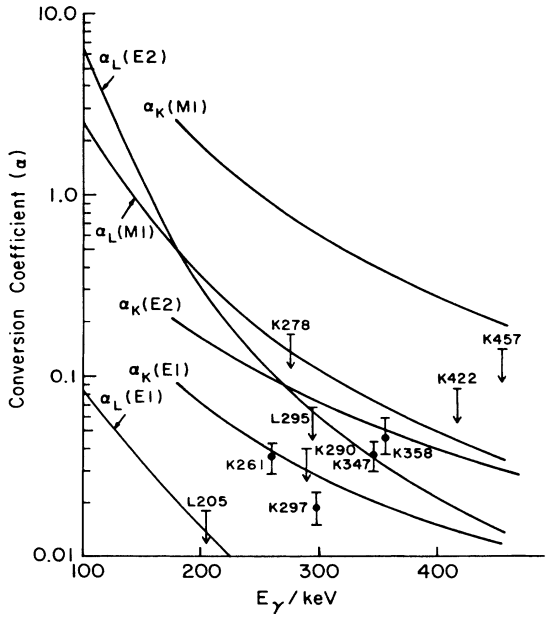

FIG. 7. Measured electron conversion coefficients compared with calculated values (Ref. 22).

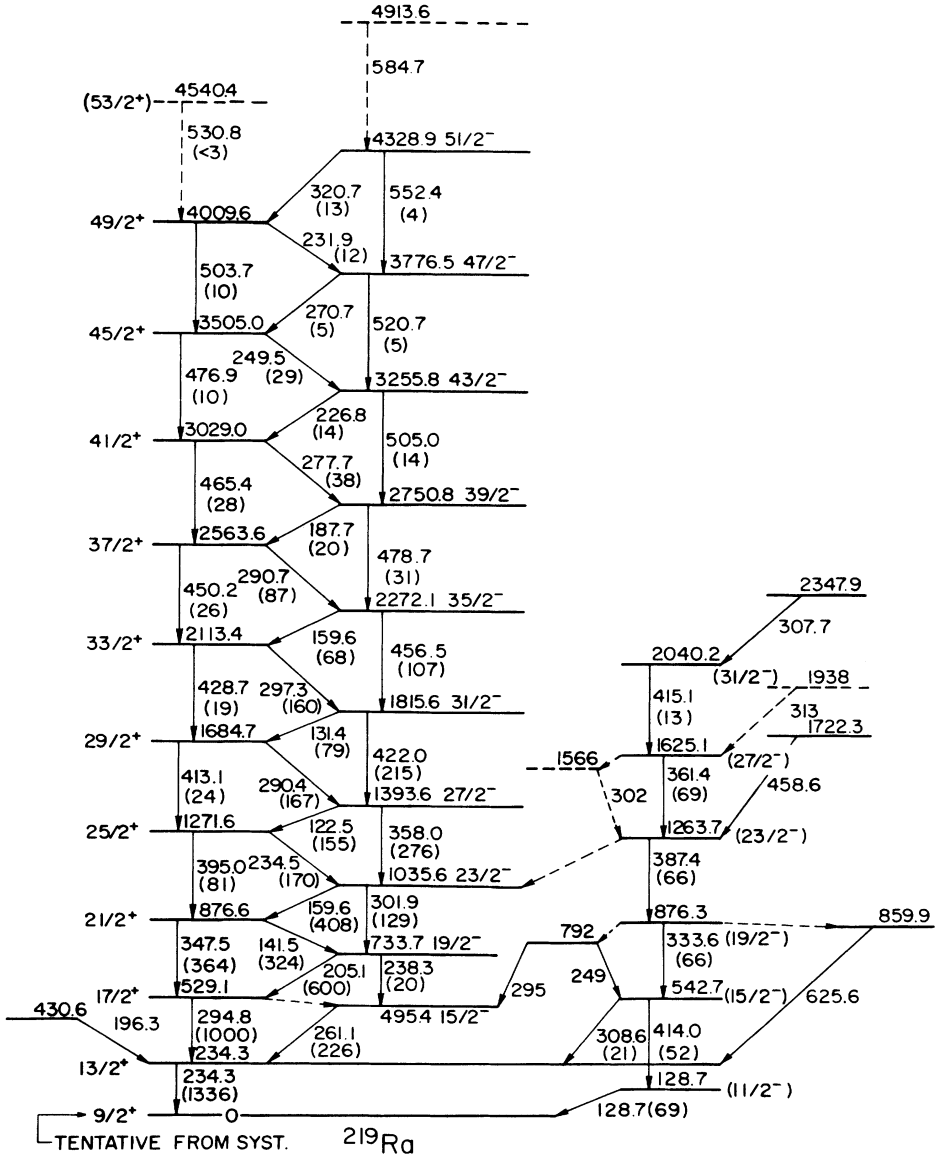

FIG. 8. Level spectrum of ^{219}Ra deduced in this work.

$B(E2)=50$ W.u., we then infer an average $B(E1)$ of 3.5×10^{-3} W.u. For the higher-lying $J^{\pi}=\frac{15}{2}^{-}$ state, we find that

$$B(E1;J\rightarrow J-1)/B(E2;J\rightarrow J-2)=1.3\times10^{-7}\ \text{fm}^{-2}\ .$$

If we again estimate $B(E2)=50$ W.u., then $B(E1)=2.2\times10^{-4}$ W.u., which implies a considerably more hindered deexcitation. Such a hindrance suggests that the $J^{\pi}=\frac{13}{2}^{+}$ and the higher-lying $J^{\pi}=\frac{15}{2}^{-}$ state have different single particle configurations and, consequently, that this $J^{\pi}=\frac{15}{2}^{-}$ state arises primarily from the $j_{15/2}$ single neutron state. Hindered $E1$ deexcitations also connect members of the $\nu j_{15/2}$ negative parity band with the $\nu g_{9/2}$ positive parity band in ^{217}Ra.

We begin a discussion of odd-A nuclei in this region with an examination of the spectra of neighboring even-even nuclei. The $A\leq220$ Ra and Th isotopes are weakly deformed, as shown by the $E(4_1^+)/E(2_1^+)$ ratios:[3–10] 1.69 for ^{216}Ra, 1.90 for ^{218}Ra, 2.30 for ^{220}Ra, 1.73 for ^{218}Th, and 2.04 for ^{220}Th [well deformed and vibrational nuclei are characterized by $E(4_1^+)/E(2_1^+)$ values of approximately 3.0 and 2.0, respectively]. Under these conditions, we would expect that a weak coupling-like model, possibly including second order effects, could account for the spectroscopy of odd-A neighbors. This hypothesis is supported by the ground state spin parities of $126\leq N\leq131$, $82\leq Z\leq89$ odd-A nuclei. Of the four odd-neutron and eight odd-proton nuclei in this group whose ground states have been studied,[15,34,36] each is reproduced by the weak coupling predictions.

We now consider the spectroscopy of four odd-A nuclei in the region: ^{217,219}Ac and ^{217,219}Ra. Figure 9 shows how these isotopes[3,5,10,33,35,37–39] conform to the general pattern associated with weak coupling. In a weak coupling model, the coupling of a state of the

TABLE II. Measured and theoretical conversion coefficients for γ rays in ^{219}Ra.

Conversion line	$\alpha_{measured}$	α_{theory} $E1$	$E2$	$M1$	Assignment
$L205$	<0.018	0.014	0.28	0.33	$E1$
$K261$	0.036(7)	0.039	0.096	0.91	$E1$
$K278$	<0.17	0.033	0.084	0.74	$E1$
$K290$	<0.040	0.030	0.078	0.67	$E1$
$K295$[a]	$=0.075$	0.029	0.075	0.64	$E2$
$L295$	<0.067	0.0053	0.064	0.115	$E2$
$K297$	0.019(4)	0.029	0.074	0.62	$E1$
$K347$	0.037(7)	0.021	0.053	0.41	$E2$
$K358$	0.046(9)	0.019	0.050	0.37	$E2$
$K422$	<0.085	0.014	0.018	0.24	$E2$
$K457$	<0.14	0.012	0.014	0.20	$E2$

[a]295 keV transition assumed $E2$ and used for normalization.

even-even core to the unpaired nucleon generates a multiplet of states having angular momenta

$$|j_{s.p.}-J_c| \leq J \leq j_{s.p.}+J_c ,$$

where $j_{s.p.}$ and J_c are the angular momenta of the single particle and core states, respectively. Of these states, only the one or two states of highest angular momentum would be strongly populated in the heavy ion fusion-evaporation reactions which have been used to study these isotopes. If the multiplet member with angular momentum

$$J_{max}=j_{s.p.}+J_c$$

has a lower excitation energy than the member having angular momentum $J_{max}-1$, only the state having $J=J_{max}$ will usually be observed. Both $J=J_{max}$ and $J=J_{max}-1$ states may be seen if the reverse is true.

We find one exception to the weak coupling pattern among the spectra displayed in Fig. 9. The band head of the negative parity band in ^{219}Ra is tentatively assigned to have $J^{\pi}=(\frac{11}{2}^-)$; the unique parity orbital in the $N>126$ neutron shell, however, is the $j_{15/2}$ one. Clearly, this state has an origin different from the classical weak coupling of a $j^{\pi}=\frac{15}{2}^-$ particle to the 0^+ ground state of the even-even core. Such a configuration of levels, called "anomalous coupling" by several authors,[40] signals that additional strength in the core-particle interaction will invalidate the weak coupling picture. Two recently studied nuclei in which anomalous coupling is observed[41,42] are ^{75}Se and ^{103}Tc.

The core-particle interaction, which is frequently expressed[1] by $Q_{core}\cdot Q_{s.p.}$, can be strengthened in several ways. The first is to increase the single particle quadrupole moment, which is given by[43]

$$Q_{s.p.}=b(N+\tfrac{3}{2})(2j_{s.p.}-1)/(2j_{s.p.}+2) ,$$

where b is a constant and N is the major oscillator shell of the valence particle. For $g_{9/2}$ and $j_{15/2}$ orbitals, this expression yields

$$Q_{s.p.}(g_{9/2})=5.5 \text{ b}$$

and

$$Q_{s.p.}(j_{15/2})=7.0 \text{ b} .$$

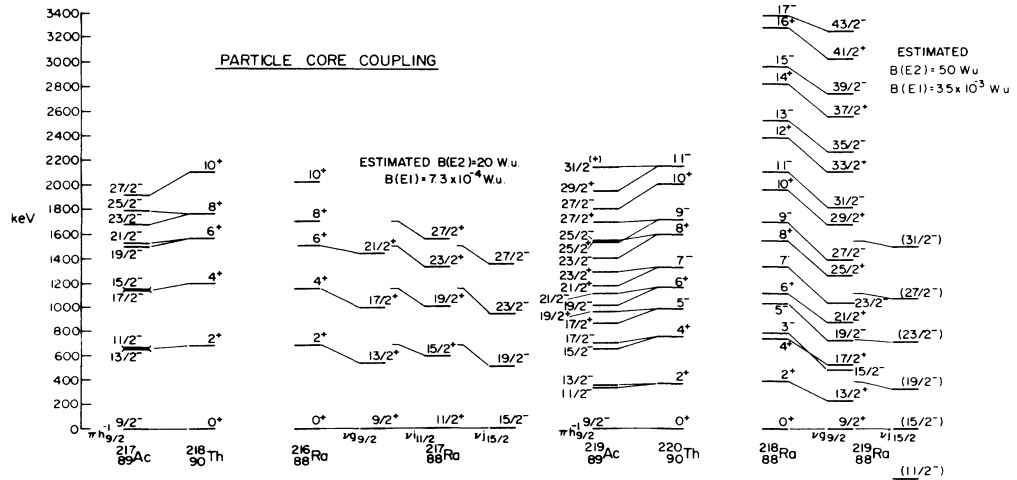

FIG. 9. Partial-core coupling behavior for $A=217$ and 219 (Refs. 3, 5, 10, 33, 35, and 37–39). Lines connect core nucleus states to corresponding weak coupling states in the odd-A nuclei. Single particle configurations are indicated under each odd-A band.

TABLE III. $B(E1{:}J\rightarrow J-1)/B(E2{:}J\rightarrow J-2)$ values in ^{219}Ra. The spin and parity of the initial state are given by J^{π}.

$2x(J^{\pi}-J_{g.s.})$	$B(E1)/B(E2)$ (10^{-6} fm^{-2})
5^-	2.52(18)
6^+	1.12(08)
7^-	1.49(10)
8^+	1.23(16)
9^-	1.16(08)
10^+	2.77(64)
11^-	1.41(9)
12^+	3.68(26)
13^-	2.14(30)
14^+	1.96(14)
15^-	1.76(18)
16^+	1.06(17)
17^-	2.08(28)
18^+	3.34(48)
19^-	1.34(42)
20^+	2.38(44)
21^-	4.01(94)
Average	2.09(9)

In this way, the $j_{15/2}$ orbital lends extra strength to the $Q_{\text{core}}\cdot Q_{\text{s.p.}}$ product.

Many treatments of particle-core coupling take pairing into account. One such treatment is that of Hagemann and Dönau,[44] which includes the pairing factor $(u_j^2-v_j^2)$ in the coupling strength. This factor would also increase the core-particle interaction of the $\nu j_{15/2}$ configuration with respect to the $\nu g_{9/2}$ one because the latter orbital is approximately half full. Theoretical investigations of anomalous coupling behavior usually invoke Pauli effects as well (see, e.g., Refs. 41 and 42).

An increase in the core deformation also increases the interaction. We would expect, for example, that the core of ^{221}Ra would be more deformed than that of ^{219}Ra. In turn, the anomalous coupling might occur in the $\nu g_{9/2}$ band. The ground state spin of $\frac{5}{2}^+$ measured[23] for ^{221}Ra could be explained in terms of the intermediate coupling of the valence neutron to a weakly deformed core (as for the $\nu j_{15/2}$ band in ^{219}Ra) instead of by the strong coupling of this neutron to a well-deformed core, as is suggested by Nazarewicz and Olanders.[45]

In Fig. 10, we demonstrate how weak coupling may also occur in ^{221}Th. Figure 10 displays[10,46] the similarity between the yrast structures of ^{220}Th and ^{221}Th. While no spin assignment for the ground state of ^{221}Th has been made, the clear correspondence between yrast states of these two nuclei strongly suggests an interpretation of the ^{221}Th spectrum in terms of the weak coupling of the odd neutron to a ^{220}Th core. Such a correspondence is no longer apparent for the observed[47,48] low spin states of ^{223}Th, a more quadrupole-deformed isotope. It seems clear that the strict weak coupling picture no longer applies in this case.

The foregoing examples suggest a more general question: for what range of β_2 is a weak coupling model appropriate? As we have noted above, the particle-core coupling behavior should depend on the single particle orbital involved. We can, however, use as a starting

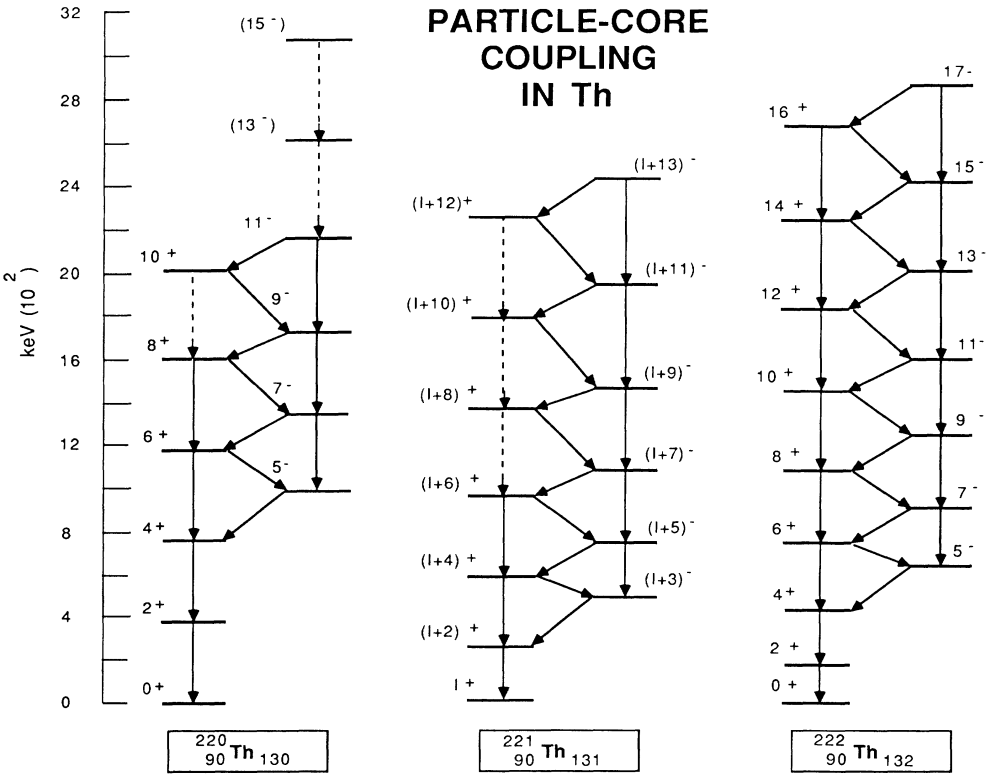

FIG. 10. Particle-core coupling behavior (Refs. 10 and 46) in ^{221}Th.

Z \ N	126	128	130	132	134
90	^{216}Th	^{217}Th	^{218}Th 0.08 (1)	^{219}Th	^{220}Th 0.10 (1)	^{221}Th	^{222}Th 0.15 (1)	^{223}Th	^{224}Th 0.17 (1)
89	^{215}Ac	^{216}Ac	^{217}Ac	^{218}Ac	^{219}Ac	^{220}Ac	^{221}Ac	^{222}Ac	^{223}Ac
88	^{214}Ra 0.05 (1)	^{215}Ra	^{216}Ra 0.08 (2)	^{217}Ra	^{218}Ra 0.09 (1)	^{219}Ra	^{220}Ra 0.14 (4)	^{221}Ra	^{222}Ra 0.19 (1)

FIG. 11. Estimated β_2 values (see text) for even-even nuclei in the mass 220 region.

point the suggestion by Ring and Schuck[40] that a weak coupling model should be appropriate when

$$\beta_2 A^{2/3} < 4 \ .$$

If we use $A = 220$, this condition yields

$$\beta_2 < 0.11 \ .$$

Clearly, this limit is no more than a rough estimate; nevertheless, it is interesting to compare this expectation to experimental results from the radium region.

In Fig. 11, we display a map of Ra, Ac, and Th isotopes and assign β_2 values to the even-A Ra and Th nuclei; this figure allows us to compare, in an approximate way, particle-core coupling behavior in the odd-A isotopes with core β_2 values. The β_2 values were calculated using the procedure described in Ref. 10 from the lifetimes of the 2_1^+ states, where available, or from the expression proposed in Ref. 10 for calculating the half-life of the 2_1^+ state from the energy of the $2_1^+ \rightarrow 0_{g.s.}^+$ transition. The procedure for calculating β_2 from $B(E2)$ uses the rigid rotor model, which is not strictly correct for all isotopes included in the figure; the results are, however, useful estimates.

The criterion proposed in Ref. 40 appears to agree with observations. As we have seen, the $\nu g_{9/2}$ bands of both ^{219}Ra and ^{221}Th can be described by a weak coupling model. In ^{221}Ra and ^{223}Th, such a description is not successful. The numerical result $\beta_2 < 0.11$ agrees with the location of this transition.

The weak coupling model can also be used (by a method similar to that used by Gai *et al.*[49]) to account for the markedly different level spectra observed[37,38] in the isobars ^{219}Ra and ^{219}Ac. When the core is prolate, weak coupling of a valence nucleon in an orbit having angular momentum $j_{s.p.}$ leads to the occurrence of the state with angular momentum $J_{max} = j_{s.p.} + J_{core}$ at a lower excitation energy than the state having $J = J_{max} - 1$ and, thus, to a band in which states of equal parity are two units of angular momentum apart. For the case of a valence hole, the expected order of the J_{max} and $J_{max} - 1$ states is reversed and a difference of only one unit of angular momentum occurs between states of equal parity.

The absence of $J_{max} - 1$ states from the observed structure of the $\nu g_{9/2}$ band in ^{219}Ra can be explained simply as the result of a particle coupling to the slightly prolate ^{218}Ra core. On the other hand, both J_{max} and $J_{max} - 1$ states of the weak coupling multiplets of ^{219}Ac are observed. This configuration can be described in the simple coupling picture as a $\pi h_{9/2}$ hole coupled to a ^{220}Th core. This picture is consistent not only with ^{219}Ac and ^{219}Ra, but also with the observed spectra[33,35] of ^{217}Ac and ^{217}Ra.

The importance of orbital occupation in weak coupling behavior is emphasized by the model presented by Hagemann and Dönau.[44] A factor arising from the pairing force is included in the core-particle interaction. In short, if the orbital is less than 50% occupied, then the weak coupling multiplet is ordered just as in the case of particle coupling; for orbit occupation of greater than 50%, the multiplet is ordered as it would be for a hole.

The Woods-Saxon deformed shell model constructed for quadrupole, octupole and hexadecapole deformations[45] provides an alternative description of ^{219}Ra and its neighbors. In the study by Nazarewicz and Olanders,[45] a calculation is presented in which both β_2 and β_4 are fixed to values ($\beta_2 = 0.15$, $\beta_4 = 0.08$) chosen to represent averages over the mass range $A = 219$–229. This calculation reproduces ground state spins measured for ^{221,223,225,227,229}Ra, ^{223}Fe, ^{225,227}Ac, and ^{227,229}Pa; in addition, it predicts that the ground state of ^{219}Ra has $J^\pi = \frac{3}{2}^+$. The prediction does not agree with the observations of Ref. 29. A value of $\beta_3 = 0.10$ is used in Ref. 45 both to reproduce the ground state spin in ^{221}Ra and to predict the ground state configuration for ^{219}Ra. The significance of this calculation may be questioned, however, because of the uncertainty[50] surrounding this assumption of large octupole deformation in the ground states of these nuclei, especially in the case of ^{219}Ra.

In conclusion, we have demonstrated that the usefulness of a weak coupling description for an odd-A nucleus depends on both the degree of deformation of the even-even core nucleus and the single particle orbital in which the unpaired nucleon is located. Furthermore, we are able to account for the strikingly different observed excitation spectra of ^{219}Ra and ^{219}Ac using such a weak coupling description.

This work was supported in part by U.S. Department of Energy Contracts DE-AC02-76ER03074 and DE-AC02-76CH00016 and by the National Science Foundation.

*Present address: Physics Department, Florida State University, Tallahassee, FL 32306.
†Present address: AT&T Bell Laboratories, 131 Morristown Road, Basking Ridge, NJ 07920.
‡Present address: Department of Physics, Tennessee Technological University, Cookeville, TN 38506.
§Present address: Research Institute of Physics, Fack, S-10405 Stockholm 50, Sweden.

[1] A. DeShalit, Phys. Rev. **122**, 1530 (1961).
[2] D. Horn, O. Häusser, B. Haas, T. K. Alexander, T. Faestermann, H. R. Andrews, and D. Ward, Nucl. Phys. **A317**, 520 (1979).
[3] A. Chevallier, J. Chevallier, B. Haas, S. Khazrouni, and N. Schulz, Z. Phys. A **308**, 277 (1982).

[4]J. Fernandez-Niello, H. Puchta, F. Riess, and W. Trautmann, Nucl. Phys. **A391**, 221 (1982).
[5]M. Gai, J. F. Ennis, M. Ruscev, E. C. Schloemer, B. Shivakumar, S. M. Sterbenz, N. Tsoupas, and D. A. Bromley, Phys. Rev. Lett. **51**, 646 (1983).
[6]Y. Gono, private communication.
[7]J. D. Burrows, P. A. Butler, K. A. Connell, A. N. James, G. D. Jones, A. M. Y. El-Lawindy, T. P. Morrison, J. Simpson, and R. Wadsworth, J. Phys. G **10**, 1449 (1984).
[8]P. D. Cottle, J. F. Shriner, Jr., F. Dellagiacoma, J. F. Ennis, M. Gai, D. A. Bromley, J. W. Olness, E. K. Warburton, L. Hildingsson, M. A. Quader, and D. B. Fossan, Phys. Rev. C **30**, 1768 (1984); J. F. Shriner, Jr., P. D. Cottle, J. F. Ennis, M. Gai, D. A. Bromley, J. W. Olness, E. K. Warburton, L. Hildingsson, M. A. Quader, and D. B. Fossan, *ibid.* **32**, 1888 (1985).
[9]A. Celler, Ch. Briancon, J. S. Dionisio, A. Lefevre, Ch. Vieu, J. Zylicz, R. Kulessa, C. Mittag, J. Fernandez-Niello, Ch. Lauterbach, H. Puchta, and F. Riess, Nucl. Phys. **A432**, 421 (1985).
[10]W. Bonin, H. Backe, M. Dahlinger, S. Glienke, D. Habs, E. Hanelt, E. Kankeleit, and B. Schwartz, Z. Phys. A **322**, 59 (1985).
[11]W. Bonin, M. Dahlinger, S. Glienke, E. Kankeleit, M. Kramer, D. Habs, B. Schwartz, and H. Backe, Z. Phys. A **310**, 249 (1983).
[12]D. Ward, G. D. Dracoulis, J. R. Leigh, R. J. Charity, D. J. Hinde, and J. O. Newton, Nucl. Phys. **A406**, 591 (1983).
[13]B. Schwartz, Ch. Ender, D. Habs, D. Schwalm, M. Dahlinger, E. Kankeleit, H. Folger, R. S. Simon, and H. Backe, Z. Phys. A **323**, 489 (1986).
[14]P. Schüler, Ch. Lauterbach, Y. K. Agarwal, J. DeBoer, K. P. Blume, P. A. Butler, K. Euler, Ch. Fleischmann, C. Günther, E. Hauber, H. J. Maier, M. Marten-Tölle, Ch. Schandera, R. S. Simon, R. Tölle, and P. Zeyen, Phys. Lett. **174B**, 241 (1986).
[15]*Table of Isotopes*, 7th ed., edited by C. M. Lederer and V. S. Shirley (Wiley, New York, 1978).
[16]J. A. Cizewski and A. E. L. Dieperink, Phys. Lett. **164B**, 236 (1985).
[17]R. F. Casten, Phys. Rev. Lett. **54**, 1991 (1985).
[18]C. Mittag, J. Fernandez-Niello, F. Riess, and H. Puchta, Ann. Israeli Phys. Soc. **7**, 277 (1984).
[19]P. D. Cottle, M. Gai, J. F. Ennis, J. R. Shriner, Jr., D. A. Bromley, C. W. Beausang, L. Hildingsson, W. F. Piel, Jr., D. B. Fossan, J. W. Olness, and E. K. Warburton, Phys. Rev. C **33**, 1855 (1986).
[20]A. Gavron, Phys. Rev. C **21**, 230 (1980).
[21]J. Van Klinken and K. Wisshak, Nucl. Instrum. Methods **98**, 1 (1972).
[22]F. Rösel, H. M. Fries, K. Alder, and H. C. Pauli, At. Data Nucl. Data Tables **21**, 292 (1978).
[23]S. A. Ahmad, W. Klempt, R. Neugart, E. W. Otten, K. Wendt, C. Ekström and the ISOLDE Collaboration, Phys. Lett. **133B**, 47 (1983).
[24]Y. A. Ellis, Nucl. Data Sheets **28**, 639 (1979).
[25]K. S. Toth and Y. A. Ellis, Nucl. Data Sheets **27**, 681 (1979).
[26]C. Maples, Nucl. Data Sheets **22**, 207 (1977).
[27]C. Maples, Nucl. Data Sheets **22**, 275 (1977).
[28]M. J. Martin, Nucl. Data Sheets **25**, 397 (1978).
[29]A. M. Y. El-Lawindy, J. D. Burrows, P. A. Butler, J. R. Cresswell, V. Holliday, G. D. Jones, R. Tanner, R. Wadsworth, D. L. Watson, K. A. Connell, J. Simpson, C. Lauterbach, and J. R. Mines, J. Phys. G **13**, 93 (1987).
[30]E. K. Warburton, J. W. Olness, C. J. Lister, R. W. Zurmuhle, and J. A. Becker, Phys. Rev. C **31**, 1184 (1985).
[31]H. J. Daley and M. Gai, Phys. Lett. **149B**, 13 (1984).
[32]G. A. Leander, W. Nazarewicz, G. F. Bertsch, and J. Dudek, Nucl. Phys. **A453**, 58 (1986).
[33]N. Roy, D. J. Decman, H. Kluge, K. H. Maier, A. Maj, C. Mittag, J. Fernandez-Niello, H. Puchta, and F. Riess, Nucl. Phys. **A426**, 379 (1984).
[34]D. J. Decman, H. Grawe, H. Kluge, and K. H. Maier, Z. Phys. A **310**, 55 (1983).
[35]D. J. Decman, H. Grawe, H. Kluge, K. H. Maier, A. Maj, N. Roy, Y. K. Agarwal, K. P. Blume, M. Guttormsen, H. Hübel, and J. Recht, Nucl. Phys. **A436**, 311 (1985).
[36]A. Coc, C. Thibault, F. Touchard, H. T. Duong, P. Juncar, S. Liberman, J. Pinard, J. Lerme, J. L. Vialle, S. Büttgenbach, A. C. Mueller, A. Pesnelle, and the ISOLDE Collaboration, Phys. Lett. **163B**, 66 (1985).
[37]S. Khazrouni, A. Chevallier, J. Chevallier, O. Helene, G. Ramanantsizehena, and N. Schulz, Z. Phys. A **320**, 535 (1985).
[38]M. W. Drigert and J. A. Cizewski, Phys. Rev. C **31**, 1977 (1985); M. W. Drigert and J. A. Cizewski, Phys. Rev. C **33**, 1344 (1986).
[39]Y. Itoh, Y. Gono, T. Kubo, M. Sugawara, and T. Nomura, Nucl. Phys. **A410**, 156 (1983).
[40]P. Ring and P. Schuck, *The Nuclear Many-Body Problem* (Springer-Verlag, New York, 1980).
[41]Y. Tokunaga, H. Seyfarth, O. W. B. Schult, S. Brant, V. Paar, D. Vretenar, H. G. Börner, G. Barreau, H. Faust, Ch. Hofmeyr, K. Schreckenbach, and R. A. Meyer, Nucl. Phys. **A430**, 269 (1984).
[42]P. DeGelder, D. DeFrenne, K. Heyde, N. Kaffrell, A. M. Van Den Berg, N. Blasi, M. N. Harakeh, and W. A. Sterrenburg, Nucl. Phys. **A401**, 397 (1983).
[43]P. J. Brussaard and P. W. M. Glaudemans, *Shell Model Applications in Nuclear Spectroscopy* (North-Holland, Amsterdam, 1977).
[44]U. Hagemann and F. Dönau, Phys. Lett. **59B**, 321 (1975).
[45]W. Nazarewicz and P. Olanders, Nucl. Phys. **A441**, 420 (1985).
[46]M. Dahlinger, E. Hanelt, K. Kankeleit, B. Schwartz, D. Schwalm, D. Habs, R. S. Simon, and H. Backe, Z. Phys. A **321**, 535 (1985).
[47]M. Dahlinger, E. Hanelt, E. Kankeleit, B. Schwartz, D. Habs, Ch. Ender, D. Schwalm, R. S. Simon, and H. Backe, GSI Annual Report 1985, p. 51.
[48]P. A. Butler *et al.*, *Nuclear Structure, Reactions and Symmetries, Vol. I*, edited by R. A. Meyer and V. Paar (World-Scientific, Singapore, 1986), p. 101.
[49]M. Gai, A. Arima and D. Strottman, in *Proceedings of the International Conference on Band Structure and Nuclear Dynamics, New Orleans, 1980*, edited by A. L. Goodman *et al.* (North-Holland, Amsterdam, 1980), Vol. 1, p. 158.
[50]W. Nazarewicz, P. Olanders, I. Ragnarsson, J. Dudek, G. A. Leander, P. Möller, and E. Ruchowska, Nucl. Phys. **A429**, 269 (1984).